The Design and Performance of Feedback Controllers for the Attenuation of Road Noise in Vehicles

Jordan Cheer and Stephen J. Elliott

Institute of Sound and Vibration Research, University of Southampton, Southampton, SO17 1BJ, UK

(Received 15 February 2013; revised 15 October 2013; accepted 16 October 2013)

Active noise control systems offer a potential method of reducing the weight of acoustic treatments in vehicles and, therefore, of increasing fuel efficiency. The commercialisation of active noise control has not been widespread, however, partly due to the cost of implementation. This paper investigates the design and performance of feedback road noise control systems, which could be implemented cost-effectively by using the car audio loudspeakers as control sources and low-cost microphones as error sensors. Three feedback control systems are investigated, of increasing complexity: a single-input single-output (SISO) controller; a SISO controller employing weighted arrays of error sensors and control sources; and a fully-coupled multi-input multi-output (MIMO) controller. For each of the three controllers robustness and disturbance enhancement constraints are defined, and by formulating the three controllers, using an Internal Model Control (IMC) architecture and using frequency discretisation, the constrained optimization problems are solvable using sequential quadratic programming. The performance of the three controllers and the associated design methods are first evaluated in a simulated environment, which allows the physical limits on performance to be understood. Finally, to validate the results in the simulated environment, the performance of the three controllers has been calculated using data measured in a car cabin, and it has been shown that the fully-coupled MIMO controller is able to achieve significant low frequency road noise control, at the expense of increased implementation complexity compared to the SISO and SISO weighted transducer arrays feedback controllers.

1. INTRODUCTION

Noise in road vehicles is widely acknowledged as one of the key factors in governing their commercial success.[1] Although passive acoustic treatments remain the dominant method of reducing both engine noise and road noise within the car cabin,[2] there has also been considerable interest in active noise control measures for both of these types of noise.[3] This interest has recently been driven by the need to improve the fuel efficiency of vehicles through the use of economical engine designs and by reducing the vehicle's weight. Economical engine designs such as variable displacement, which usually operates by deactivating a number of cylinders, often result in increased low frequency noise. Similarly, reducing the weight of a vehicle also results in increased low frequency noise. Low frequency noise is difficult to control using lightweight passive measures, and since active noise control systems are most effective at low frequencies and may be implemented within a car with relatively little increase in weight, they offer a convenient complementary solution. This is particularly true when the active noise control systems are integrated into the vehicle's electronic systems, for example, by employing the car audio loudspeakers.[4]

Low frequency engine noise has been successfully controlled using feedforward control systems employing an engine speed reference signal, low cost microphone error sensors, and the car audio loudspeakers as control sources.[5] In a feedforward control system, as illustrated in Fig. 1(a), the control signal is generated by filtering the reference signal, x, which is correlated with the noise to be controlled, with filters that are adapted to minimise the error signals. A number of commercial feedforward engine noise control systems have been implemented due to their relatively low-cost.[6–10] Reducing the weight of vehicles also increases the low frequency noise produced in the car cabin due to road-tyre interactions. Road noise has also been controlled using a feedforward control system,[11] however, due to the random nature of road noise and the complex propagation path between structural excitation of the tyre and the acoustic noise produced in the car cabin, the implementation of a feedforward controller is significantly more demanding. Reference signals for a feedforward road noise control system have been obtained from accelerometers mounted to the vehicle's suspension and bodywork,[11] however, in order to obtain sufficient coherence between the reference and disturbance signals it is necessary to employ at least six accelerometers.[11,12] Although a feedforward control system has been reported to achieve A-weighted noise level reductions of up to 7 dB at the driver's ear position between 100 and 200 Hz,[11] the need for multiple reference accelerometers means that the system is relatively expensive to implement and, therefore, has seen limited commercial implementation.

As a result of the high cost of a feedforward road noise control system, there is interest in implementing road noise cancellation using a feedback system, as this avoids the need for separate reference sensors. In a feedback control system, the control signals are produced by directly filtering the error signals, as shown in Fig. 1(b), which results in different performance characteristics compared to a feedforward controller.[13,14] Feedback control of road noise has been the focus of research presented by Adachi and Sano, for example,[14,15] which led to a mass-production system implemented in the

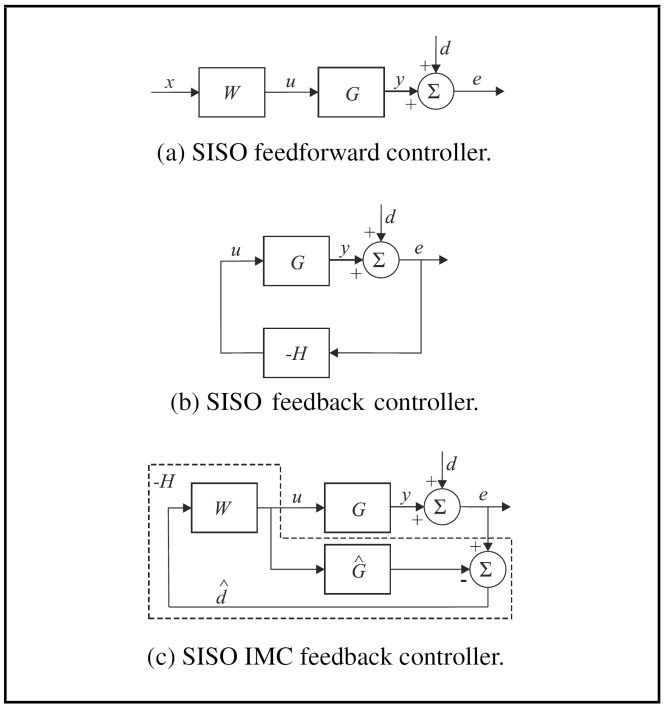

Figure 1. Block diagrams of (a) the standard SISO feedforward controller; (b) the standard SISO feedback controller; (c) the IMC SISO feedback controller.

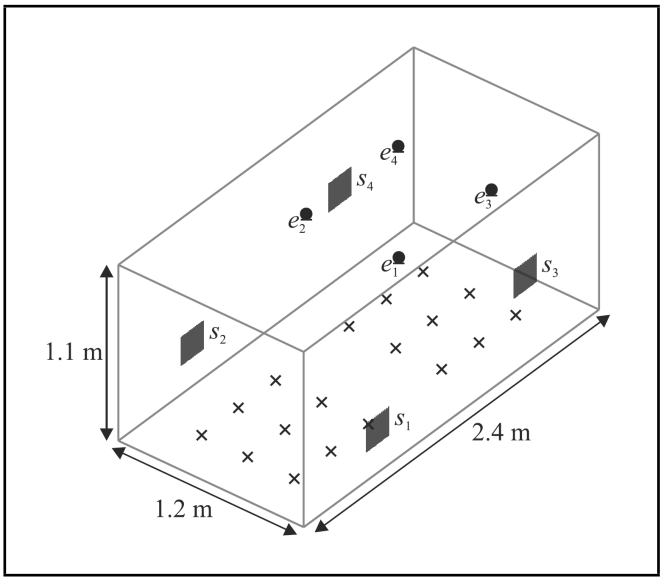

Figure 2. Car cabin sized rectangular enclosure showing locations of the 18 primary structural excitations (×), 4 microphones, 4 control sources (solid rectangles), and the enclosure dimensions.

Honda Accord estate car.[4] This single channel control system achieves 10 dB reduction in a narrowband 40 Hz boom in the front seats, which corresponds to the first longitudinal enclosure mode of this vehicle, whilst avoiding enhancements in the rear seat positions.

A control system combining feedforward engine noise control and feedback road noise control could potentially be implemented at a very low cost. Modern car audio systems increasingly include a large number of loudspeakers, digital signal processing, and even microphones for communication and audio system monitoring. If a combined engine and road noise control system were integrated with such an audio system, then the cost of implementation would be very low and would largely be related to the software implementation of the controllers. Due to the potentially cost-effective nature of feedback road noise control, this paper investigates the design and performance of feedback control systems of varying complexity. In Section 2, a simulated active road noise control problem is defined, which will be used to investigate the design and performance of the feedback control strategies and provide a context within which the physical limits on the controllers' performance can be understood. In Section 3, the design of a single-input single-output (SISO), Internal Model Control (IMC) controller is presented, and its performance limitations are highlighted through simulation results. A multi-source, multi-sensor SISO controller is presented in Section 4, which is based on the spatial and temporal filtering method described by Cheer and Elliott.[16] However, a novel method of formulating this controller, using IMC to minimise the sum of the squared error signals directly, is presented here. In Section 5, a fully coupled multi-input, multi-output (MIMO) controller is presented, and its performance is evaluated in the simulated environment. Finally, the three feedback control strategies are applied to real road noise data in offline simulations, which highlight the potential performance of the three control systems in Section 6.

2. ACTIVE NOISE CONTROL PROBLEM DEFINITION

To evaluate the performance limitations of the feedback control systems, it is convenient to employ a modelled acoustic environment. This allows the physical limits on the control systems to be clearly understood, without the complexities of a real car geometry. The performance of the feedback control systems will initially be investigated in a flexible walled rectangular enclosure, whose dimensions are similar to those of a car cabin, as shown in Fig. 2. The walls modelled here are assumed to be constructed from plywood panels with a Young's modulus of 5×10^9 Nm^{-2}, a thickness of 12 mm, a Poisson ratio of 0.3, a density of 465 kgm^{-3}, and a damping ratio of 0.05. Although the flat shape and material properties of these walls are clearly not the same as those in a practical vehicle, it has been found that the essential nature of the acoustic-structural interaction is similar. The enclosure has been modelled using the modal model of structural-acoustic coupling,[17–19] and the primary disturbance has been produced by 18 uncorrelated structural excitations on the floor of the enclosure, as shown by the crosses in Fig. 2. This provides a control scenario that simulates the road noise control problem, in which the flexible structure of the car cabin is excited by multiple uncorrelated excitations from the interaction between the road, the four tyres, and the automobile's structure.

The aim of this paper is to investigate cost-effective road noise control systems, and, therefore, although higher levels of control will certainly be achievable by employing loudspeakers in close proximity to the car cabin's occupants, the investigated control systems will only employ the four standard low frequency car audio loudspeakers. The assumed positions of these loudspeakers in the rectangular enclosure are shown by the grey rectangles in Fig. 2.

The general aim of the feedback control strategies is to minimise the sound pressure levels, due to road noise, that the car cabin occupants are subject to. To evaluate this criterion and to also provide error signals, four microphone positions have been defined in the rectangular enclosure, as shown in Fig. 2.

These microphones are positioned at the front and rear seat headrest positions.

3. SINGLE-INPUT SINGLE-OUTPUT CONTROL

Single-input, single-output feedback control systems have been widely studied in the context of dynamic systems, and the performance limitations are well documented.[20,21] Although such controllers have been successfully applied in active noise cancelling headphones and headrests,[22] their application to active road noise systems is limited to the control of single, problematic, acoustic modes.[4,14,15] Therefore, it is interesting to first consider the performance limitations on the SISO control system shown in Fig. 1(b) when the system is optimised to minimise a single error signal.

3.1. Controller Formulation

The response of the closed-loop feedback controller in Fig. 1(b) is governed by the sensitivity function

$$S(j\omega) = \frac{e(j\omega)}{d(j\omega)} = \frac{1}{1 + G(j\omega)H(j\omega)}; \tag{1}$$

where $e(j\omega)$ is the error signal, $d(j\omega)$ is the disturbance signal, $G(j\omega)$ is the plant response, $H(j\omega)$ is the response of the feedback controller, j is $\sqrt{-1}$, and ω is the angular frequency. There are a number of methods of designing the feedback controller, $H(j\omega)$.[20,21] By using the IMC architecture presented in Fig. 1(c), the feedback control problem is reformulated as an equivalent feedforward controller,[20,23] and the optimization of the controller becomes a convex problem.[22] The IMC formulation is also of significant benefit in designing the two feedback control systems investigated in the following sections and, therefore, for consistency, will also be employed for the SISO system.

The response of the IMC feedback controller, which is contained within the dashed lines in Fig. 1(c), is given by

$$H(j\omega) = -\frac{W(j\omega)}{1 + \hat{G}(j\omega)W(j\omega)}; \tag{2}$$

where $W(j\omega)$ is the control filter response, and $\hat{G}(j\omega)$ is the modelled plant response. If it is assumed that the plant model is perfect, i.e. $\hat{G}(j\omega) = G(j\omega)$, then the sensitivity function becomes

$$S(j\omega) = 1 + G(j\omega)W(j\omega); \tag{3}$$

and the controller is purely feedforward.

3.2. Design Objectives

The aim of the SISO controller is to minimise the modulus squared error signal, and this cost function can be written as

$$J(j\omega) = |1 + G(j\omega)W(j\omega)|^2 S_{dd}(j\omega); \tag{4}$$

where $S_{dd}(j\omega) = E\left(|d(j\omega)|^2\right)$ is the power spectrum of the disturbance signal, and E denotes the expectation operator.

Under the assumption that the plant model is perfect, then the optimum controller is a purely feedforward system with a perfect reference signal provided by d. In this case, the optimum control filter, W, that minimises the cost function given by Eq. (4) can be calculated using standard Wiener methods.[20] However, in a real system, the plant response will not be perfectly modelled, and this will result in a degree of feedback in the system. This leads to potential stability and disturbance enhancement issues and the need to enforce robust stability and out-of-band enhancement constraints in the controller design process.

For the SISO feedback controller, robust stability can be enforced by assuming that the true plant response can be represented using the multiplicative uncertainty model,[20] so that $G(j\omega) = G_0(j\omega)(1+\Delta_G)$, where $|\Delta_G| \leq B(j\omega)$. The robust stability condition is then given by

$$|T(j\omega)|B(j\omega) < 1 \quad \text{for all} \quad \omega; \tag{5}$$

where $B(j\omega)$ is the maximum value of the plant uncertainty and $T(j\omega)$ is the complementary sensitivity function, which is equal to $-G(j\omega)W(j\omega)$ for the SISO IMC controller. When designing a feedback controller, it is often desirable to also limit the maximum enhancement in the disturbance signal. For the SISO controller, a constraint on the maximum enhancement can also be imposed by limiting the sensitivity function, given by Eq. (3), to be less than a maximum value of A. This constraint can be expressed as[18,20]

$$|S(j\omega)|\frac{1}{A} < 1 \quad \text{for all} \quad \omega. \tag{6}$$

3.3. Controller Optimization

The design of the SISO IMC feedback controller requires the minimisation of the cost function in Eq. (4), whilst maintaining the robust stability and disturbance enhancement constraints given by Eqs. (5) and (6), respectively. A similar design problem has been discussed by Rafaely and Elliott,[22] and their optimization method will be employed here.

If the control filter, W, is implemented as an I coefficient, Finite Impulse Response (FIR) filter, $\mathbf{w}$, then the cost function given by Eq. (4) is quadratic with respect to the filter coefficients. The optimization of the control filter coefficients is therefore a constrained minimisation problem, and previous work has shown that it is useful to set up this convex optimization in the discrete frequency domain.[24] If the frequency responses of the plant and controller are discretized at K linearly spaced frequencies, k, then the optizmisation of the SISO IMC controller can be expressed as

$$\begin{aligned} \min_{\mathbf{w}} \quad & \frac{1}{K}\sum_{k=k_1}^{k_2} |1 + G(k)W(k)|^2 S_{dd}(k); \\ \text{subject to} \quad & |G(k)W(k)|B(k) < 1 \quad \text{for all} \quad k; \\ & |1 + G(k)W(k)|\frac{1}{A} < 1 \quad \text{for all} \quad k; \end{aligned} \tag{7}$$

where k_1 and k_2 define the upper and lower bounds of the bandwidth over which disturbance attenuation is required. These bounds may be used to both limit the optimization space, and to ensure that the controller does not attempt to produce a small zone of control at the error sensor.[25] This optimization problem has been solved using sequential quadratic programming, which is possible since the cost function is convex and the constraints are affine,[26] although, other programming methods may also be used.[22]

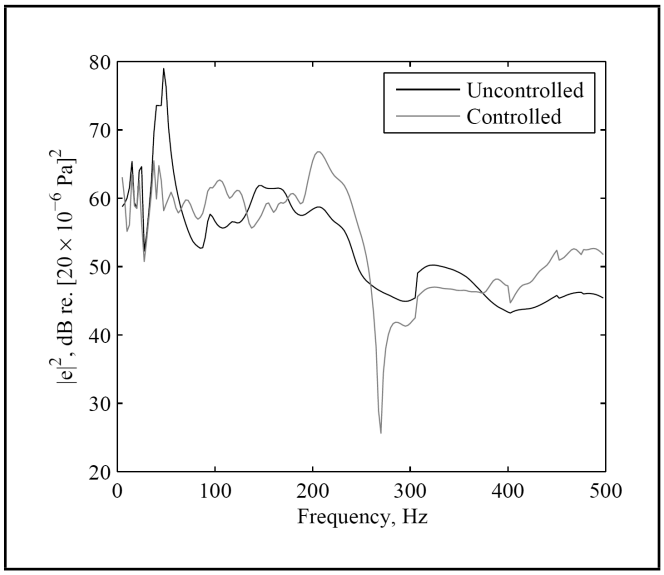

Figure 3. The error signal from microphone 2 before and after control using the SISO IMC feedback controller.

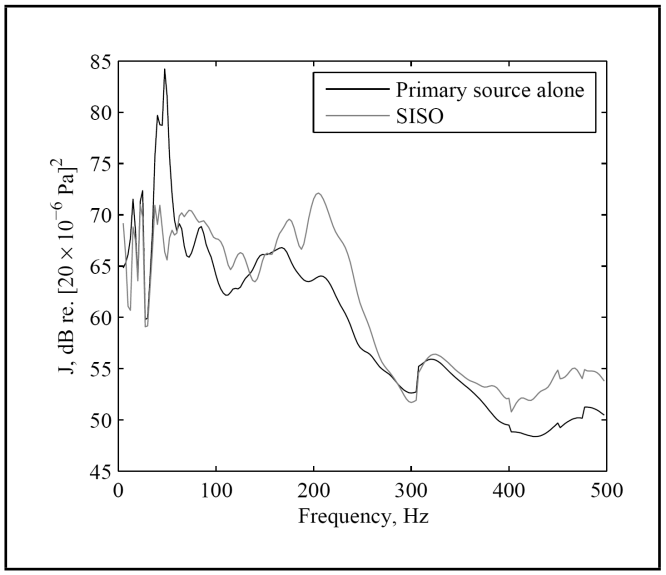

Figure 4. The sum of the squared pressures at the four headrest microphones before and after control using the SISO IMC feedback controller.

To ensure that the solution to the discrete problem given by Eq. (7) approximates the desired solution to the continuous problem, it is important that K is large enough, such that the discretized frequency responses are accurately represented. This can be achieved by ensuring that the impulse responses of the discretized responses have negligible amplitude at the end of their responses.[22] It is also important to ensure that the FIR control filter, $\mathbf{w}$, is sufficiently long such that the obtained solution is optimal, and this can be ensured by gradually increasing the length of $\mathbf{w}$ until there is no further improvement in performance.[27]

3.4. Performance

In the car cabin environment, a reasonable objective of the SISO feedback controller is to minimise the pressure at the driver's ear position. The SISO feedback controller for this application will use microphone 2, positioned at the driver's right ear, as the error sensor and source 2, which is the closest source to the driver, as the control source. The frequency responses have been discretized at $K = 198$ frequencies at a sample rate of 1 kHz, and the bandwidth of control has been defined between 0 and 200 Hz by setting $k_1 = 0$ and $k_2 = 200$. The robust stability constraint has been set to B=0.5, which gives a gain margin of around 3.5 dB and a phase margin of 40°, and the disturbance enhancement constraint has been set to $A = 2$, which ensures a maximum enhancement in the squared pressure of 6 dB. An $I = 64$ coefficient control filter has been optimised using this method and the resulting change in the error signal, which is the pressure at microphone 2, is shown in Fig. 3. The uncontrolled field is generated by driving all 18 structural excitations in Section 2 with uncorrelated white noise signals.

From the change in the error signal shown in Fig. 3 it can be seen that at the resonance at around 50 Hz, which is dominated by the radiation from the $(1, 2)$ structural mode of the floor panel, the disturbance signal is attenuated by around 15 dB and some further reductions are achieved at around 150 Hz and 320 Hz. It can also be seen that the enhancement constraint ensures that the maximum level of enhancement at any frequency is 6 dB. Although significant control has been achieved at the 50 Hz resonance, the bandwidth of control of the SISO controller is limited due to the delay between the error sensor and control source.[20]

To determine the effect of the SISO control system on the pressures at the positions of the other car cabin occupants, Fig. 4 shows the sum of the squared pressures calculated at the four headrest microphones before and after control. From this plot, it can be seen that although significant levels of control of the resonance at 50 Hz are still achieved, no significant control is achieved at higher frequencies, and at around 200 Hz there is a 10 dB enhancement in the sum of squared pressures. The limited control achieved by the SISO controller at the other headrest positions can be related to both the use of a single error sensor and a single control source. The SISO controller is neither able to observe or control multiple modes of the enclosure and, therefore, only achieves significant control at low frequencies, where the response is dominated by a single acoustic mode and produces significant enhancements at higher frequencies, where multiple modes are excited but not observed by the single sensor. This is consistent with the observations of Sano et al.[4] and also highlights the physical limitations on control using a single source and sensor control system, although the enhancements are limited in[4] through the use of a secondary control loop.

4. SINGLE-INPUT SINGLE-OUTPUT CONTROL WITH WEIGHTED TRANSDUCER ARRAYS

To improve the performance of a feedback control system it is necessary to employ multiple sensors, to improve observation and multiple sources, to improve control. Although this may be achieved through a fully MIMO feedback controller, the design and implementation is significantly more demanding than for a SISO controller. Therefore, the performance of a SISO controller employing the weighted sum of multiple error sensors and control sources, as shown in Fig. 5(a), will be investigated. The use of multiple sensors and sources in single channel control systems has previously been inves-

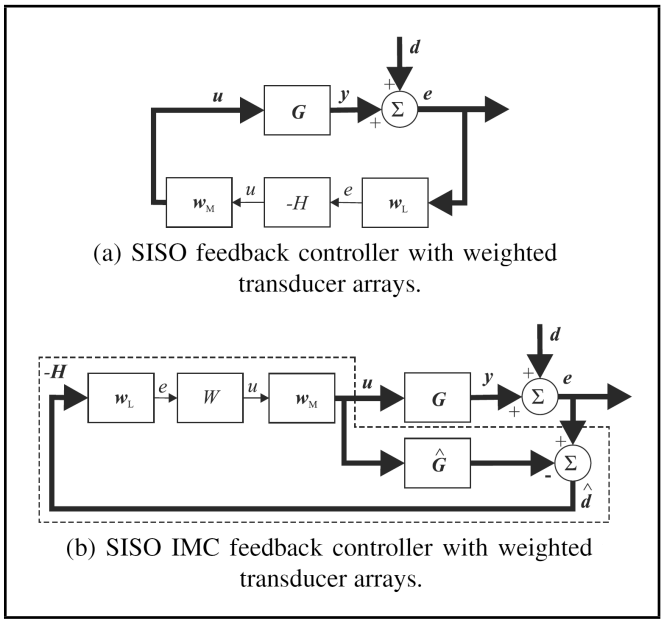

Figure 5. Block diagrams of the SISO (a) and IMC SISO (b) feedback controllers with weighted transducer arrays.

tigated in the context of modal control.[28] The following sections present a new method of simultaneously optimising the SISO feedback controller, $H(j\omega)$, and the transducer weightings, $\mathbf{w}_L$ and $\mathbf{w}_M$.

4.1. Controller Formulation

The proposed control system shown in Fig. 5(a) consists of L error sensors and M control sources. A single composite error signal, $e(j\omega)$, is generated through the weighted summation of the error signals from the L error microphones. This weighted summation is implemented via the $(L \times 1)$ vector of real, frequency independent, error sensor weightings, $\mathbf{w}_L$, and can be expressed in terms of the $(L \times 1)$ vector of pressures at the error sensors, $\mathbf{e}(j\omega)$, as

$$e(j\omega) = \mathbf{w}_L^T \mathbf{e}(j\omega) = \mathbf{w}_L^T \left(\mathbf{d}(j\omega) + \mathbf{G}(j\omega)\mathbf{u}(j\omega)\right); \quad (8)$$

where ^{T} denotes the transpose operator, $\mathbf{d}(j\omega)$ is the $(L \times 1)$ vector of disturbance signals, $\mathbf{G}(j\omega)$ is the $(L \times M)$ matrix of plant responses, and $\mathbf{u}(j\omega)$ is the $(M \times 1)$ vector of control signals. The vector of control signals is generated from the single composite control signal, $u(j\omega)$, via the vector of real, frequency independent, source weightings, $\mathbf{w}_M$, as

$$\mathbf{u}(j\omega) = \mathbf{w}_M u(j\omega). \quad (9)$$

Using Eqs. (8) and (9), and the relationship between the composite error and the composite control signals, $u(j\omega) = -H(j\omega)e(j\omega)$, it can be shown that $G(j\omega) = \mathbf{w}_L^T \mathbf{G}(j\omega)\mathbf{w}_M$, and so the SISO sensitivity function between the composite error and disturbance signals is

$$S(j\omega) = \frac{e(j\omega)}{d(j\omega)} = \frac{\mathbf{w}_L^T \mathbf{e}(j\omega)}{\mathbf{w}_L^T \mathbf{d}(j\omega)} = \frac{1}{1 + \mathbf{w}_L^T \mathbf{G}(j\omega)\mathbf{w}_M H(j\omega)}. \quad (10)$$

In this case, the design of the feedback controller is dependent on both the feedback controller, $H(j\omega)$, and the transducer weightings, $\mathbf{w}_M$ and $\mathbf{w}_L$. Previous systems employing transducer weightings for acoustical control problems have largely employed a two-step procedure, in which the transducer weightings are first defined, and then the SISO feedback controller is designed.[16,29] However, by formulating the control problem using an IMC architecture, the design problem can be transformed into a convex optimization problem in which the control filter and transducer weightings can be optimised in parallel.

It has been shown by Cheer[18] that the SISO controller with weighted transducer arrays can be formulated in two different ways using the IMC architecture. The first formulation, in which the transducer weightings are included in the plant modelling path, leads to the minimisation of the weighted error signal, $e(j\omega)$. The second formulation, in which the transducer weightings are included in the control path, leads to the minimisation of the physical error signals and, therefore, provides a better practical solution.[18] This IMC formulation is shown in Fig. 5(b).

The response of the IMC feedback controller, which includes the multichannel transducer weightings, plant response model and SISO control filter and is contained within the dashed lines in Fig. 5(b), is given in this case by

$$\mathbf{H}(j\omega) = -\left[\mathbf{I} + \mathbf{w}_M W(j\omega)\mathbf{w}_L^T \hat{\mathbf{G}}(j\omega)\right]^{-1} \mathbf{w}_M W(j\omega)\mathbf{w}_L^T; \quad (11)$$

where $\hat{\mathbf{G}}(j\omega)$ is the $(M \times L)$ matrix of modelled plant responses. If it is again assumed that the plant model is perfect, i.e. $\hat{\mathbf{G}}(j\omega) = \mathbf{G}(j\omega)$, then the sensitivity function of the IMC feedback controller is

$$\mathbf{S}(j\omega) = \mathbf{I} + \mathbf{G}(j\omega)\mathbf{w}_M W(j\omega)\mathbf{w}_L^T; \quad (12)$$

and the controller is again entirely feedforward with a controller response given by $\mathbf{w}_M W(j\omega)\mathbf{w}_L^T$.

4.2. Design Objectives

The aim of the multi-sensor feedback controller is to minimise the sum of the squared error signals. This cost function can be expressed as

$$J(j\omega) = \text{trace}\left[E\left(\mathbf{e}(j\omega)\mathbf{e}^H(j\omega)\right)\right]; \quad (13)$$

and since the vector of error signals is given by $\mathbf{e}(j\omega) = \mathbf{S}(j\omega)\mathbf{d}(j\omega)$, this cost function can be expressed as

$$\begin{aligned} J(j\omega) = \text{trace}\big[& \\ & \mathbf{G}(j\omega)\mathbf{w}_M W(j\omega)\mathbf{w}_L^T \mathbf{S}_{dd}(j\omega)\mathbf{w}_L W^*(j\omega)\mathbf{w}_M^T \mathbf{G}^H(j\omega) + \\ & \mathbf{G}(j\omega)\mathbf{w}_M W(j\omega)\mathbf{w}_L^T \mathbf{S}_{dd}(j\omega) + \\ & \mathbf{S}_{dd}(j\omega)\mathbf{w}_L W^*(j\omega)\mathbf{w}_M^T \mathbf{G}^H(j\omega) + \mathbf{S}_{dd}(j\omega)\ \big]; \end{aligned} \quad (14)$$

where $\mathbf{S}_{dd}(j\omega)$ is the matrix of power and cross spectral densities of the primary disturbance. From Eq. (14) it can be seen that the IMC formulation leads to a quadratic cost function with respect to both the control filter, $W(j\omega)$, and the transducer weightings. This design problem may therefore be solved using the frequency discretized convex optimization approach employed for the SISO controller.

To design a practical SISO controller with weighted transducer arrays, it is again necessary to enforce a robust stability constraint. In this case, although the control filter remains SISO, the response of the controller is governed by the matrix

sensitivity function given by Eq. (12). Therefore, it is necessary to obtain a robust stability design constraint for the MIMO system. Although there are some limitations in the case of a MIMO system,[30] it is again assumed that the plant uncertainty can be modelled using multiplicative output uncertainty, so that the condition for robust stability is given by[30]

$$\bar{\sigma}\left(\mathbf{T}(j\omega)\right) B(j\omega) < 1 \quad \text{for all} \;\; \omega; \tag{15}$$

where $\bar{\sigma}$ indicates the maximum singular value, and $\mathbf{T}(j\omega)$ is the complementary sensitivity function given by $-\mathbf{G}(j\omega)\mathbf{w}_M W(j\omega)\mathbf{w}_L^T$ in this case.

In designing the feedback controller, it is again desirable to also enforce a constraint on the maximum enhancement in the disturbance signal. In the case of the multi-sensor system, there are a number of possible constraints, which have been discussed by Cheer.[18] For the active noise control application, however, constraining the maximum enhancement in the individual error signals provides a more uniform reduction in the pressure by avoiding high levels of enhancements at some error sensors being balanced out by reductions at other sensors.[18] This constraint on the enhancement in the individual disturbance signals may be expressed as

$$\max\left[\text{diag}\left(\mathbf{D}(j\omega)\mathbf{S}(j\omega)\mathbf{S}_{dd}(j\omega)\mathbf{S}^H(j\omega)\right)\right] \frac{1}{A} < 1 \quad \text{for all} \;\; \omega; \tag{16}$$

where

$$\mathbf{D}(j\omega) = \begin{bmatrix} \frac{1}{E|d_1(j\omega)|^2} & 0 & 0 & 0 \\ 0 & \frac{1}{E|d_2(j\omega)|^2} & 0 & 0 \\ 0 & 0 & \ddots & 0 \\ 0 & 0 & 0 & \frac{1}{E|d_L(j\omega)|^2} \end{bmatrix}; \tag{17}$$

and the maximum enhancement in the L magnitude squared disturbance signals will be less than a maximum value defined by A.

4.3. Controller Optimization

The design of the SISO IMC feedback controller with weighted transducer arrays requires the minimisation of the cost function in Eq. (14), whilst maintaining the robust stability and enhancement constraints given by Eqs. (15) and (16), respectively. If the control filter, W, is implemented as an I coefficient FIR filter, $\mathbf{w}$, and the frequency responses are discretized at K linearly spaced frequencies, the optimization of the controller can be achieved using the convex optimization method described in Section 3.3.

The discrete frequency optimization problem for the SISO IMC controller with weighted transducer arrays can be expressed as

$$\begin{aligned} \min_{\mathbf{w},\mathbf{w}_L,\mathbf{w}_M} \quad & \frac{1}{K}\sum_{k=k_1}^{k_2} \text{trace}\big[\\ & \mathbf{G}(j\omega)\mathbf{w}_M W(j\omega)\mathbf{w}_L^T \mathbf{S}_{dd}(j\omega)\mathbf{w}_L W^*(k)\mathbf{w}_M^T \mathbf{G}^H(k) + \\ & \mathbf{G}(k)\mathbf{w}_M W(k)\mathbf{w}_L^T \mathbf{S}_{dd}(k) + \\ & \mathbf{S}_{dd}(k)\mathbf{w}_L W^*(k)\mathbf{w}_M^T \mathbf{G}^H(k) + \mathbf{S}_{dd}(k)\,\big]; \\ \text{subject to} \quad & \bar{\sigma}\left(\mathbf{T}(k)\right) B(k) < 1 \quad \text{for all} \;\; k; \\ & \max\left[\text{diag}\left(\mathbf{D}(k)\mathbf{S}(k)\mathbf{S}_{dd}(k)\mathbf{S}^H(k)\right)\right] \frac{1}{A} < 1 \quad \text{for all} \;\; k. \end{aligned} \tag{18}$$

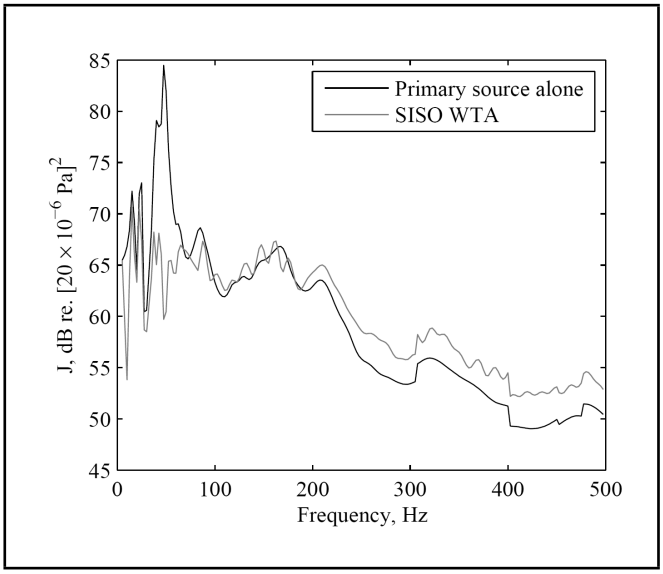

Figure 6. The sum of the squared pressures at the four headrest microphones before and after control using the SISO IMC feedback controller with weighted transducer arrays (WTA).

This optimization problem has again been solved using sequential quadratic programming, and it is again important to define the frequency discretisation, K, and the control filter length, I, such that the solution is close to the optimal continuous domain solution, as described in Section 3.3.

4.4. Performance

In the car cabin environment, the aim of the road noise controller is to minimise the pressures at the headrest positions, and for the system to be cost-effective, it is desirable for the controller to employ the car audio loudspeakers. The control system has therefore been defined using the four error microphones and the four control sources shown in Fig. 2.

The optimization problem has again been discretized at $K = 198$ frequencies, and the bandwidth of control has been defined between 0 and 200 Hz. The robust stability constraint has been defined as $B = 0.5$, and the enhancement constraint has been set to $A = 4$, which gives a maximum enhancement in the squared disturbance signals of 6 dB. An $I = 64$ coefficient control filter has been optimised along with the transducer weightings, and the resulting change in the cost function, given by the sum of the squared error signals at the four headrest microphones, is shown in Fig. 6.

From the simulation results presented in Fig. 6, it can be seen that the controller has achieved significant reductions in the cost function at the 50 Hz resonance. Reductions of around 3 dB are also achieved at 85 Hz, which corresponds to the first longitudinal acoustic mode of the enclosure that has been increased from the 71 Hz rigid-walled enclosure mode due to the structural-acoustic coupling. At frequencies above 200 Hz, it can be seen that the controller produces enhancements in the cost function of less than 6 dB, which is a result of the enforced enhancement constraint. Comparing these results to those shown in Fig. 4 for the SISO controller, it can be seen that the most significant improvement achieved by the multi-sensor, multi-source controller is to constrain the maximum enhancement levels. However, despite the use of multiple sources and sensors, the bandwidth over which significant attenuation is achieved is still rather limited, and this is due to

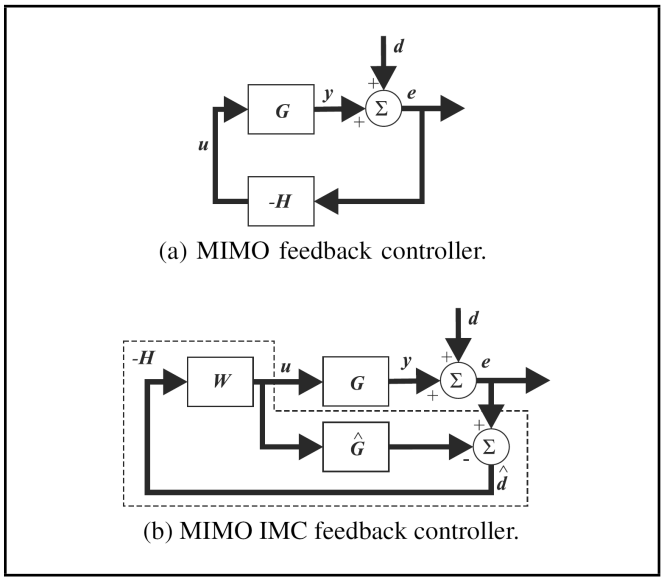

(a) MIMO feedback controller.

(b) MIMO IMC feedback controller.

Figure 7. Block diagrams of the MIMO (a) and IMC MIMO (b) feedback controllers.

the inability of a SISO controller to control the response of the enclosure when there is any significant modal overlap, so only the relatively isolated resonance at 50 Hz is significantly controlled.

5. MULTI-INPUT, MULTI-OUTPUT CONTROL

Although the SISO controller with weighted transducer arrays has shown improvements compared to the SISO controller, it does not provide a wide control bandwidth. Therefore, it is interesting to investigate the potential performance of a fully coupled MIMO feedback controller. Mutlichannel feedback control has been widely investigated, and a wide variety of optimal design processes have been described.[30] The application of a MIMO feedback controller to the road noise control problem has been suggested,[13] however, the performance of such a controller has not been presented. The design and performance of a MIMO feedback controller, as shown in Fig. 7(a), will be investigated in the following sections.

5.1. Controller Formulation

The MIMO feedback control system shown in Fig. 7(a) consists of L error sensors and M control sources, which may also be employed by a feedforward engine noise control system. In the case of the MIMO system, the sensitivity function which governs the closed-loop response is given by

$$\mathbf{S}(j\omega) = \left[\mathbf{I} + \mathbf{G}(j\omega)\mathbf{H}(j\omega)\right]^{-1}; \tag{19}$$

where $\mathbf{H}(j\omega)$ is the L input, M output feedback controller. Although there are a large number of methods of designing MIMO feedback controllers,[30] it is again convenient to use the IMC formulation of the MIMO controller shown in Fig. 7(b), due to its relative simplicity from a designers perspective.[22]

The response of the IMC feedback controller shown in Fig. 7(b), which is contained within the dashed lines, is given by

$$\mathbf{H}(j\omega) = -\left[\mathbf{I} + \mathbf{W}(j\omega)\hat{\mathbf{G}}(j\omega)\right]^{-1}\mathbf{W}(j\omega); \tag{20}$$

where $\mathbf{W}(j\omega)$ is the frequency response of the L input, M output control filter. Assuming once again that the modelled plant response is perfect, then the sensitivity function of the MIMO IMC controller is

$$\mathbf{S}(j\omega) = \mathbf{I} + \mathbf{G}(j\omega)\mathbf{W}(j\omega). \tag{21}$$

5.2. Design Objectives

The aim of the MIMO feedback controller is again to minimise the sum of the squared error signals, which is given by Eq. (13). For the fully-coupled MIMO controller, this cost function can be expressed using the sensitivity function given by Eq. (21) as

$$\begin{aligned} J(j\omega) = \mathrm{trace}\big[&\mathbf{G}(j\omega)\mathbf{W}(j\omega)\mathbf{S}_{dd}(j\omega)\mathbf{W}^H(j\omega)\mathbf{G}^H(j\omega) + \\ &\mathbf{G}(j\omega)\mathbf{W}(j\omega)\mathbf{S}_{dd}(j\omega) + \\ &\mathbf{S}_{dd}(j\omega)\mathbf{W}^H(j\omega)\mathbf{G}^H(j\omega) + \mathbf{S}_{dd}(j\omega)\,\big]. \end{aligned} \tag{22}$$

This cost function is quadratic, and the unconstrained, nominal solution can be obtained using the standard Wiener methods. However, the robust stability constraint given for the MIMO case by Eq. (15) must again be upheld, where the complementary sensitivity function for the fully-coupled MIMO IMC system is $\mathbf{T}(j\omega) = -\mathbf{G}(j\omega)\mathbf{W}(j\omega)$. The disturbance enhancement constraint for the MIMO IMC controller is identical to that described in Section 4.2 and given by Eq. (15), however, the sensitivity function is now given by Eq. (21).

5.3. Controller Optimization

The design of the MIMO IMC feedback controller requires the minimisation of the cost function given by Eq. (22), whilst the robust stability and disturbance enhancement constraints are maintained. If the control filter matrix, $\mathbf{W}$, is implemented as an ML bank of FIR filters each with I coefficients and the design problem is discretized in the frequency domain at K linearly spaced frequencies, then the MIMO IMC controller can be optimised using the same convex method used above.

The discrete frequency optimization problem for the MIMO IMC controller is given by

$$\begin{aligned} \min_{\mathbf{w}} \quad & \frac{1}{K}\sum_{k=k_1}^{k_2} \mathrm{trace}\big[\mathbf{G}(k)\mathbf{W}(k)\mathbf{S}_{dd}(k)\mathbf{W}^H(k)\mathbf{G}^H(k) + \\ & \mathbf{G}(k)\mathbf{W}(k)\mathbf{S}_{dd}(k) + \mathbf{S}_{dd}(k)\mathbf{W}^H(k)\mathbf{G}^H(k) + \mathbf{S}_{dd}(k)\,\big]; \\ \text{subject to} \quad & \bar{\sigma}\left(\mathbf{T}(k)\right)B < 1 \quad \text{for all} \quad k; \\ & \max\big[\mathrm{diag}\big(\mathbf{D}(k)\mathbf{S}(k)\mathbf{S}_{dd}(k)\mathbf{S}^H(k)\big)\big]\,\frac{1}{A} < 1 \quad \text{for all} \quad k; \end{aligned} \tag{23}$$

where $\mathbf{w}$ is now the MLI vector containing all MLI filter coefficients. This optimization problem has again been solved using sequential quadratic programming, and it is again important to define the frequency discretisation, K, and the control filter length, I, such that the solution is close to the optimal continuous domain solution, as described in the previous sections.

5.4. Performance

To provide a direct comparison with the SISO controller with weighted transducer arrays, the fully-coupled MIMO controller aims to minimise the pressures at the four headrest

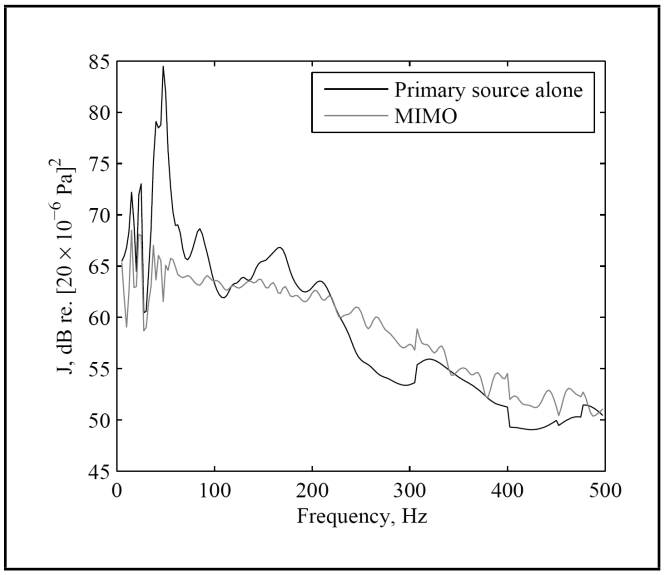

Figure 8. The sum of the squared pressures at the four headrest microphones before and after control using the MIMO IMC feedback controller.

microphones using the four control sources in Fig. 2. The fully-coupled MIMO IMC feedback controller optimization has again been discretized at $K = 198$ frequencies, and the bandwidth of control has been defined between 0 and 200 Hz. The robust stability and disturbance enhancement constraints have been defined as $B = 0.5$ and $A = 4$, and the ML bank of filters have been implemented using $I = 64$ coefficients; for the (4×4) controller this results in a total of 1024 optimization parameters compared to the 72 necessary in the SISO IMC controller with weighted transducer arrays. Figure 8 shows the change in the cost function due to the optimised MIMO IMC controller.

From the simulation results presented in Fig. 8, it can be seen that the fully-coupled MIMO controller achieves some control at the headrest positions at frequencies up to around 200 Hz. At higher frequencies, the enhancements in the cost function are limited to a similar level as was observed for the SISO controller with weighted transducer arrays, which is because both controllers use identical error sensor arrays and, therefore, have the same level of observability. However, by using a MIMO controller, the level of controllability has been increased, and, therefore, despite using the same four control sources, a higher number of modes are controllable, and the bandwidth of control is increased.

It is also important to consider the effect of the controller on the sound field at positions remote from the error sensors, since the car cabin occupants have two ears and are likely to move about in the car cabin. Therefore, the pressure has been calculated before and after control at four additional positions, corresponding to the opposite side of each of the four headrests to the error sensors in Fig. 2. The change in the sum of the squared pressures at all eight positions has then been calculated, and it has been found that control is only achieved up to around 150 Hz. Additionally, enhancements in the sum of the squared pressures of up to 9 dB are produced above this frequency. These enhancements could be limited by reducing the bandwidth over which the controller attempts to achieve attenuation, by setting $k_2 = 150$ in the optimization for example.

6. VALIDATION OF THE FEEDBACK CONTROLLERS USING DATA MEASURED IN A CAR CABIN

To validate the simulation results presented in the previous section and to highlight the potential performance of a fully-coupled MIMO feedback road noise controller in a practical car cabin environment, a series of measurements have been conducted in a small city car. The plant response has been measured between the four standard car audio loudspeakers and four headrest microphones. The primary disturbance, $\mathbf{d}$, has been measured when the car is driven at 50 km/h over a pave road surface, which gives an indication of the worst case scenario.

The three controllers have been designed according to the associated methods defined in the previous sections; that is, by minimising a specified cost function whilst maintaining both robustness and enhancement constraints. The design problem in each case has been discretized at 513 frequencies between 0 Hz and the Nyquist frequency of 1.28 kHz, and a bandwidth of control has been defined between 80 and 185 Hz to target a broadband peak in the road noise disturbance spectrum. The filter length in each case has been defined as $I = 64$.

Figure 9 shows the sum of the squared A-weighted pressures at the four headrest microphones, when there is no control and when the performance of the three controllers has been calculated using offline predictions. These offline predictions use the measured disturbance signals and plant responses, and the controlled pressures are calculated assuming linear superposition. From the thin grey line in Fig. 9, it can be seen that the SISO controller achieves almost no attenuation in the sum of the squared error signals, but does produce significant levels of enhancement. This is consistent with the simulation results presented in Fig. 4 where attenuation was only achievable where a single dominant resonance occured, and in the practical small car cabin, such isolated resonances do not occur due to both the higher number of resonances and the careful design of its response.

The thin black line in Fig. 9 shows the predicted performance of the SISO controller with weighted transducer arrays in the car cabin. From this result, it can be seen that reductions in the sum of the squared error signals of up to 3 dB have been achieved between 80 and 185 Hz, while the enhancements are significantly lower than for the SISO controller. Finally, the thick grey line in Fig. 9 shows the predicted performance of the fully-MIMO controller. From this result, it can be seen that the cost function has been reduced by up to 7 dB and an average reduction over the target bandwidth of around 4 dB has been achieved. These results are consistent with the simulation results and highlight the need for a higher order control system to control road noise.

Although significant attenuations in the sum of the squared error signals are shown in Fig. 9 for the MIMO controller, it is important to consider some potential limitations of this controller. Firstly, the controllers have each been optimised for a single road noise condition, and although their response to this condition is sufficient to achieve the levels of control shown in Fig. 9 for the pave road surface, in practice, it may be necessary to adapt the control filter coefficients in real-time in order to provide control on different road surfaces. This adaptation, however, is known to be a slow process for a broadband dis-

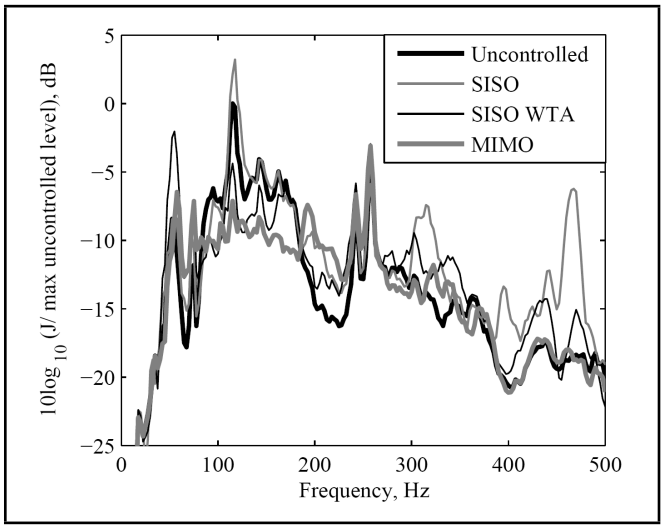

Figure 9. The sum of the squared A-weighted pressures at the four headrest microphones before control and after control using the SISO, SISO WTA and MIMO control systems.

turbance such as road noise.[20] Additionally, it is important to consider the subjective benefits provided by the controllers even under the optimal conditions presented in Fig. 9. The MIMO controller does achieve significant attenuation of the broadband peak between 80 and 185 Hz, which is a particular problem in this vehicle on this road surface; however, this attenuation comes at the expense of enhancements between 180 and 240 Hz. Although these enhancements are produced over a frequency band where the initial level is relatively low and may therefore be a worthwhile trade-off, this is a question of subjective assessment and is not straightforward to predict. Despite these limitations, the results presented in Fig. 9 highlight the potential of different feedback control configurations, which are certainly practical for a specific low frequency boom type application.

7. CONCLUSIONS

This paper has investigated the design and performance of feedback controllers for the attenuation of low frequency road noise in car cabins. Three feedback control systems have been considered: a SISO controller using a single error sensor and control source; a SISO controller using weighted arrays of error sensors and control sources; and a fully-coupled MIMO controller using multiple error sensors and control sources. To understand the physical limitations on control performance, the three controllers have been evaluated for a simple model of the road noise control problem, in which the car cabin is modelled as a flexible-walled rectangular enclosure, and the road noise disturbance is modelled as 18 uncorrelated structural excitations. Finally, the simulation results are validated by offline predictions of the control performance calculated using measurements conducted in a small city car.

The SISO feedback controller with a single error sensor positioned at the driver's right ear and a single control source located at the front nearside car audio loudspeaker position has been shown to offer some significant reductions in the pressure at the error sensor in the simualted car cabin environment. However, it has also been shown that the sum of the squared pressures at the four headrest positions is enhanced by up to 10 dB, and the SISO system is only able to achieve control at all headrest positions when the enclosure response is dominated by a single acoustic mode. The sound field inside the cabin of a small car cabin, in practice, is not dominated by a single acoustic mode and, therefore, the SISO controller is not predicted to achieve very much attenuation but does produce significant enhancements.

To overcome some of the limitations of the SISO controller, a SISO controller employing multiple error sensors and control sources is described. The SISO controller with multiple sources and sensors employs both spatial filtering, via transducer weighting functions, and temporal filtering, via the feedback control filter. A novel method of optimising the SISO control filter and the transducer weightings in parallel has been described based on an IMC formulation of the controller and frequency discretisation of the optimization problem. Additionally, a novel constraint on the enhancements in the individual error sensor pressures has been presented. The performance of the proposed control method has been calculated in both the simulated car cabin environment and the real car cabin, when a control system consisting of four headrest error sensors and four control sources positioned at the car audio loudspeaker positions has been optimised. From these results, it has been shown that the proposed system is able to achieve some low frequency attenuation whilst effectively limiting the out-of-band enhancements, however, the predicted levels and bandwidth of control are still somewhat limited as the SISO controller is only able to achieve control when there is a low modal overlap.

Although the use of a fully-coupled MIMO feedback controller for road noise control has previously been suggested,[13] no indication of the potential performance has, up to now, been presented. Therefore, using the same four headrest error sensors and the four standard car audio loudspeaker positioned sources, the performance of a fully-coupled MIMO controller has been calculated in the simulated and practical car cabin environments. From these results, it has been predicted that the fully-coupled MIMO controller would be able to achieve control up to around 200 Hz, while the out-of-band enhancements are limited by the defined enhancement constraint. The disadvantage of a MIMO controller is the additional complexity of its implementation, in this case, requiring the real-time implementation of 1024 filter coefficients, compared with 72 coefficients for the SISO case with weighted arrays and 64 coefficients for the original SISO controller. A practical implementation would also need to account for the inevitable delay through the digital controller, although simulations suggest that delays of two samples (2 ms) in the controller reduces the performance of the MIMO controller over the control bandwidth by less than 1 dB.

ACKNOWLEDGMENT

This work has been supported by the Green City Car Project, part of the 7th Framework Programme (FP7).

REFERENCES

[1] Wang, X. Rationale and history of vehicle noise and vibration refinement, *Vehicle Noise and Vibration Refinement*, Wang, X. Ed., Woodhead Publishing, Cambridge, 3–17, (2010).

[2] Vigé, D. Vehicle interior noise refinement – cabin sound package design and development, *Vehicle Noise and Vibration Refinement*, Wang, X. Ed., Woodhead Publishing, Cambridge, 286–317, (2010).

[3] Elliott, S. J. Active noise and vibration control in vehicles, *Vehicle Noise and Vibration Refinement*, Wang, X. Ed., Woodhead Publishing, Cambridge, 235–251, (2010).

[4] Sano, H., Inoue, T., Takahashi, A., Terai, K., and Nakamura, Y. Active control system for low-frequency road noise combined with an audio system, *IEEE Transactions on Speech and Audio Processing*, **9**, 775–763, (2001).

[5] Elliott, S. J., Stothers, I. M., Nelson, P., McDonald, M. A., Quinn, D. C., and Saunders, T. J. The active control of engine noise inside cars, *Proc. of INTER-NOISE 88*, **2**, Poughkeepsie, New York, 987–990, (1988).

[6] Honda, 2005 honda accord hybrid sedan interior, Retrieved from `http://www.honda.com/newsandviews/article.aspx?id=2004091736965`, (Accessed October 8, 2012).

[7] Ogawa, K. Toyota cuts 'muffled noise' in crown hybrid, Retrieved from `http://techon.nikkeibp.co.jp/english/NEWS_EN/20080619/153489/`, (Accessed October 8, 2012).

[8] Trout, C. GM shows off terrain suv with noise cancellation, says silence equals fuel efficiency, Retrieved from `http://www.engadget.com/2011/02/25/gm-shows-off-terrain-suv-with-noise-cancellation-says-silence-e/`, (Accessed October 8, 2012).

[9] Acura, Acura tsx video: Active sound control, Retrieved from `http://www.acura.com/Innovations.aspx#/Active-Sound-Control`, (Accessed October 8, 2012).

[10] Schirmacher, R., Kunkel, R., and Burghardt, M. Active noise control for the 4.0 TFSI with cylinder on demand technology in Audi's S-series, SAE Technical Paper, 2012-01-1533, (2012).

[11] Sutton, T. J., Elliott, S. J., McDonald, A. A., and Saunders, T. J. Active control of road noise inside vehicles, *Noise Control Engineering Journal*, **42**, 137–146, (1994).

[12] Oh, S. H., Kim, H. S., and Park, Y. Active control of road booming noise in automotive interiors, *Journal of the Acoustical Society of America*, **111** (1), 180–188, (2002).

[13] Elliott, S. J. and Sutton, T. Performance of feedforward and feedback systems for active control, *IEEE Transactions on Speech and Audio Processing*, **4**, 214–223, (1996).

[14] Adachi, S. and Sano, H. Application of two-degree-of-freedom type active noise control using IMC to road noise inside automobiles, *Proc. of the 35th IEEE Conference on Decision and Control*, Kobe, Japan, 2794–2795, (1996).

[15] Adachi, S. and Sano, H. Active noise control system for automobiles based on adaptive and robust control, *Proc. of the 1998 IEEE International Conference on Control Applications*, Trieste, Italy, 1125–1129, (1998).

[16] Cheer, J. and Elliott, S. J. Spatial and temporal filtering for feedback control of road noise in a car, *Proc. of the 19th International Congress on Sound and Vibration*, Vilnius, Lithuania, (2012).

[17] Dowell, E. H. and Voss, H. M. The effect of a cavity on panel vibration, *AIAA Journal*, **1** (2), 476–477, (1963).

[18] Cheer, J. Active Control of the Acoustic Environment in an Automobile Cabin, PhD thesis, University of Southampton, Southampton, UK, (2012).

[19] Cheer, J. and Elliott, S.J. The effect of structural-acoustic coupling on the active control of sound in vehicles, *Proc. of Eurodyn 2011*, Leuven, Belgium, (2011).

[20] Elliott, S. J. *Signal Processing for Active Control*, Academic Press, London, (2001).

[21] Franklin, G. F., Powell, J. D., and Emami-Naeini, A. *Feedback Control of Dynamic Systems*, Addison-Wesley, Massachusetts, (1991), 2nd ed.

[22] Rafaely, B. and Elliott, S. J. H_2/H_∞ active control of sound in a headrest: Design and implementation, *IEEE Transactions on Control System Technology*, **7**, 79–84, (1999).

[23] Morari, M. and Zafiriou, E. *Robust Process Control*, Prentice Hall, London, (1989).

[24] Boyd, S., Balakrishnan, V., Barratt, C., Khraishi, N., Li, X., Meyer, D., and Norman, S. A new CAD method and associated architectures for linear controllers, *IEEE Transactions on Automatic Control*, **33**, 268–283, (1988).

[25] Garcia-Bonito, J. and Elliott, S. J. Local active control of diffracted diffuse sound fields, *Journal of the Acoustical Society of America*, **98** (2), 1017–1024, (1995).

[26] Boyd, S. and Vandenberghe, L. *Convex Optimization*, Cambridge University Press, Cambridge, (2004).

[27] Titterton, P. and Olkin, J. A practical method for constrained-optimization controller design: H_2 or H_∞ optimization with multiple H_2 and/or H_∞ constraints, *Proc. of the 29th Asilomar Conference on Signals, Systems and Computers*, Pacific Grove, USA, 1265–1269, (1995).

[28] Meirovitch, L. *Dynamics and Control of Structures*, Wiley-Interscience, New York, (1990).

[29] Lane, S. A., Clark, R. L., and Southward, S. C. Active control of low frequency modes in an aircraft fuselage using spatially weighted arrays, *Journal of Vibration and Acoustics*, **122**, 227–233, (2000).

[30] Skogestad, S. and Postlethwaite, I. *Multivariable Feedback Control, Analysis and Design*, John Wiley & Sons, Chichester, UK, (1996).